Int. J. Heat Mass Transfer. Vol. 31, No. 2, pp. 407–417, 1988
Printed in Great Britain

0017–9310/88 $3.00 + 0.00

Augmentation of convective and boiling heat transfer by applying an electro-hydrodynamical liquid jet

AKIRA YABE
Mechanical Engineering Laboratory, Ministry of International Trade and Industry, Tsukuba Science City, Ibaraki 305, Japan

and

HIROSHI MAKI
Science University of Tokyo, Noda, Chiba 278, Japan

(*Received* 7 *September* 1987)

Abstract—The augmentation effects of an electro-hydrodynamical (EHD) liquid jet on convective and boiling heat transfer were experimentally and theoretically analyzed. The EHD liquid jet, which was the jet flow ejected through the ring electrode in the direction away from the plate, was produced by applying a high electric voltage between the ring electrode and the plate electrode. The convective heat transfer from the plate electrode was enhanced over 100 times by the forced convection and the turbulent effects of the EHD liquid jet. For the boiling heat transfer, the mean bubble detachment period was decreased, and the critical heat flux was enhanced over two times.

1. INTRODUCTION

THE ELECTRO-HYDRODYNAMICAL (EHD) phenomena researched so far for the enhancement of heat transfer can be classified into the effects for gases and the effects for liquids. The main effect of EHD phenomena in gases is the augmentation of convective heat transfer by the corona wind, which is caused by applying high electric fields to bring about corona discharges in a non-uniform electric field region close to a needle or wire electrode. Since the velocity of the corona wind reaches about 2 m s^{-1} in air, the corona wind is applicable to locally focused cooling and the augmentation of evaporation. It is also applicable to the cooling of the complicated curved passages, which is difficult when using fans. The mechanism of the corona wind has already been quantitatively made clear [1–3] and is briefly explained as follows. The ions, which are produced by ionization of a gas and have the same polarity as the needle or the wire electrode, drift in the electric field under the Coulomb force to the plate electrode without recombination. During the movement to the plate electrode, the ions transfer their momentum to neutral molecules through collisions, and the bulk flow of neutral molecules is generated.

Concerning the EHD phenomena in liquids, the existence of a gas–liquid interface changes the augmentation phenomena greatly. In the case of heat transfer accompanying phase change or including a gas–liquid interface, the surface instability due to electric fields becomes important for augmenting phase change heat transfer. As a typical example of this kind of augmentation method for condensation heat transfer, the EHD liquid extraction phenomenon in a non-uniform electric field, first observed by one of the authors, was utilized to remove condensate from the condensation surface by a helical wire to achieve a thinner condensate film for making the augmentation of condensation heat transfer. Furthermore, another EHD surface instability of the thin liquid film in a uniform electric field was utilized simultaneously to achieve EHD pseudo-dropwise condensation with negligibly small electric power consumption. At present, this EHD augmentation method is being researched to develop a high performance condenser, which is called the 'EHD condenser', for the practical application of making a high efficiency and high temperature heat pump system [4–7]. In the case of the augmentation of boiling heat transfer, the instability of the vapor–liquid interface was increased by electric fields to obtain larger critical boiling heat flux [8–10].

On the other hand, convective heat transfer in liquids without a gas–liquid or liquid–liquid interface has not yet been successfully augmented to any large degree [11]. The convection caused by the corona discharge in liquids is also effective [12], but the corona discharge in a liquid is not practically useful due to the degradation of the heat transferring medium. In the case that the temperature distribution is established in liquids, which means that the heat transfer is generated, the gradient of electrical conductivity is also produced by the temperature distribution. The electrical space charges are then created in order to

NOMENCLATURE

c_p specific heat at constant pressure
D distance between electrodes
d wire diameter composing ring electrode
E electric field strength
E_0 characteristic electric field strength, Φ/D
f_0 body force on fluid by electric field
Pr Prandtl number
p pressure
q boiling heat flux
Re_{EHDJET} EHD jet Reynolds number, $U_{EHDJET} \cdot d/\nu$
r radial axis
T temperature
ΔT temperature difference or wall superheat, $|T_\infty - T_w|$
t_b mean bubble detachment period
t_e relaxation time of electric charge, ε/σ_e
U_{EHDJET} characteristic velocity of EHD jet, $(\Phi/D) \cdot [(\varepsilon-\varepsilon_0)(\varepsilon+2\varepsilon_0)/6\varepsilon_0\rho]^{0.5}$
u velocity
u' velocity fluctuation
W inner diameter of ring electrode
W_l distance between wire electrodes (longer distance)
W_s distance between wire electrodes (shorter distance)
z vertical axis.

Greek symbols
α heat transfer coefficient
ε dielectric constant
ε_0 dielectric constant for vacuum
ε_q exchange coefficients
ε_t eddy viscosity
λ thermal conductivity
ν kinematic viscosity
ρ density of liquid
ρ_e electric charge density
σ_e electrical conductivity
Φ applied voltage or electric potential
∇ gradient.

Superscript
non-dimensionalized or time average.

Subscripts
r r-direction
z z-direction
∞ main flow region.

satisfy the continuity equation of the current. Therefore, the Coulomb force was exerted on the space charges to produce the convection effective for heat transfer augmentation. However, the produced velocity in this case would be less than a few centimeters per second [13]. Furthermore, charge injection from the surface of the electrode without any electrical discharge could occur [14, 15], and then the Coulomb force was exerted on the injected space charges. Generally, the body force f_e that acts on a fluid under the influence of electric fields is expressed by [16]

$$\mathbf{f}_e = \rho_e \mathbf{E} - (1/2)E^2\nabla\varepsilon + (1/2)\nabla[E^2\rho(\partial\varepsilon/\partial\rho)]. \quad (1)$$

In liquids, all the terms of f_e that are Coulomb force (first term), force due to the spatial gradient of dielectric constant (second term) and the electrostriction force caused by the inhomogeneity of the electric field strength (third term), are all effective and important, and consequently many kinds of EHD convection are supposed to occur.

Many experiments have been conducted by the authors which focused on the convection in liquids. Consequently, by applying a high electric voltage between the ring electrode and the parallel opposed plate electrode in the liquid mixture of R 113 and ethanol, it was found by the authors that the liquid jet was created from the center of the ring electrode in the direction away from the plate electrode, even in the case where there was no temperature distribution. Then by analyzing the EHD liquid jet in detail, it was clarified theoretically that the mechanism was the flow caused by the electrostriction force without any electrical discharges. Furthermore, it was made clear experimentally that the velocity of the flow exceeds 1 m s^{-1}. This phenomenon was named the 'EHD liquid jet' [17].

In this paper, this EHD liquid jet was applied to the heat transfer augmentation of convection and boiling, and the enhanced rate was analyzed experimentally and theoretically. Practical applications of this EHD liquid jet are: (1) convective heat transfer augmentation for heat exchangers of organic liquids, (2) the realization of the compact and high performance boiling heat exchangers for energy conservation technology and electronic cooling devices, and (3) the boiling heat transfer augmentation for the evaporators in spacecraft.

2. EXPERIMENTAL APPARATUS

The experimental apparatus for convective heat transfer augmentation is shown in Fig. 1. The heat transfer surface had a diameter of 50 mm, was made of brass, and was set inside an acrylic plastic vessel. The heat transfer surface was heated from the back by a sheath heater or cooled by the cooling water. A small area 5 mm in diameter was selected to be equal to the inner diameter of the ring electrode to measure the local heat transfer coefficients around the axisymmetric axis and was surrounded by a 2 mm thick

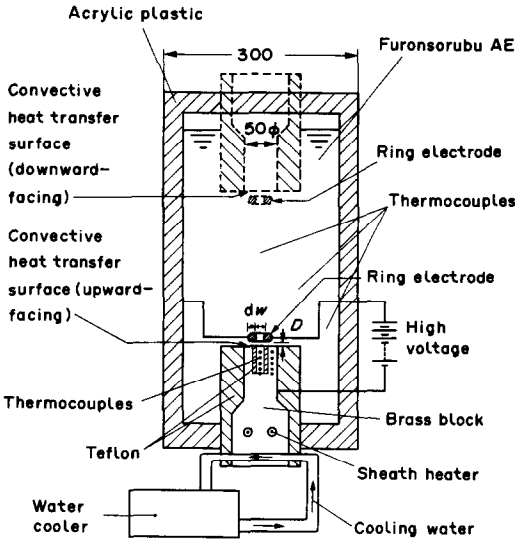

FIG. 1. Experimental apparatus for convective heat transfer augmentation.

thermal insulator made of teflon. The heat flux was measured by five K type sheath thermocouples 0.5 mm in diameter embedded in a brass block with a separation distance of 5 mm along the vertical axis. A brass ring 1 mm thick, 5.2 mm i.d., and 9 mm o.d. was added to the surface of the thermal insulator adjacent to the liquid to make a continuous metal plate electrode. But, since the ring was separated from the heat transfer surface around the axisymmetric axis by 0.1 mm, the measured heat transfer rates were not affected by conduction to the surrounding brass plate. The thermal conductivity of the brass, measured by the laser flask method, was 92.0 $W\,m^{-1}\,K^{-1}$.

An azeotropic mixture of R 113 (96 wt.%) and ethanol (4 wt.%), called Furonsorubu AE, was selected as the heat transferring liquid. Since the velocity of the EHD liquid jet was increased by the increase of electrical conductivity of liquids and was saturated for electrical conductivity beyond 3×10^{-9} $(\Omega\,m)^{-1}$ [17], the above Furonsorubu AE was selected to satisfy the saturation condition. The electrical conductivity of this liquid was nearly constant during experiments and its value was about 2×10^{-8} $(\Omega\,m)^{-1}$.

The ring electrode and the plate electrode were arranged (Fig. 1) to make an axisymmetric phenomenon, that was preferable for theoretical analysis. The ring electrode was made of 5 mm diameter copper wire and had a 5 mm i.d. and 15 mm o.d. As for the distance between electrodes D, the condition of $D = 3.5$ mm was mainly used. This is why the velocity of the EHD liquid jet was a function of D and why the velocity was highest and nearly constant between $D = 3$–4 mm [17]. Concerning the electric field, a high voltage d.c. was applied between the ring electrode and the plate electrode. This plate electrode was also used as the heat transfer surface on the condition that it was made a cathode and electrically earthed.

The heat transfer surface faced both upward and downward by changing the flange as shown in Fig. 1. The velocity distribution was measured by a laser Doppler velocimeter (DANTEK 55N20 Tracker). Submicrometer diameter powder of molecular sieve 4A was selected as the seeding material for LDV. Furthermore, the turbulent intensity was measured by analyzing the signals of the LDV with an analyzing recorder (YOKOGAWA 3655E).

The experimental apparatus used for boiling heat transfer augmentation was similar to the apparatus in Fig. 1 with the heat transfer surface facing upward [18]. In order to make one apparent vapor column on the boiling surface and to investigate the effect of electric fields on the bubble detachment period, the diameter of the boiling heat transfer surface, made of copper, was selected as 5 mm. This would be smaller than the critical wavelength for the Taylor instability of the vapor–liquid interface if the applied voltage is below 10 kV. The heat transfer surface was surrounded by the teflon thermal insulator. The surface of the boiling heat transfer was surrounded by a 1 mm thermal insulating layer made of epoxy resin and connected to a surrounding outer plate electrode which was 130 mm in diameter. The copper block was heated from below by an electric sheath heater, but most of the heat was removed by the forced convection of oil just above the heating part to realize the transition boiling stably on the boiling heat transfer surface. The average bubble detachment period was measured by high speed pictures of 2000 frames per second taken by a high speed video system (KODAK SP2000).

3. AUGMENTATION OF CONVECTIVE HEAT TRANSFER BY APPLYING AN EHD LIQUID JET

3.1. *Relationship between convective heat transfer and an electric field*

In Fig. 2, the relationship between the augmented convective heat transfer coefficients and the electric field strength are shown. The applied voltage and also the characteristic electric field strength, the applied voltage divided by the electrode distance D, are shown on the abscissa. From an analytical point of view, the electric field strength is more important than the applied voltage, but to explain by distinct values, the applied voltage is used as the parameter of the electric field in the following figures and explanations. From the figure, it is seen that the heat transfer coefficients are increased in proportion to the applied voltage. The augmented heat transfer coefficients in the case of the upward-facing heated plate were almost equal to those in the case of the downward-facing cooled plate. Also, the heat transfer coefficients in the case of the upward-facing cooled plate were almost equal to those in the case of the downward-facing heated plate. But the heat transfer coefficients obtained for the cases of the upward-facing heated plate and the downward-facing cooled plate were about 50% greater than those

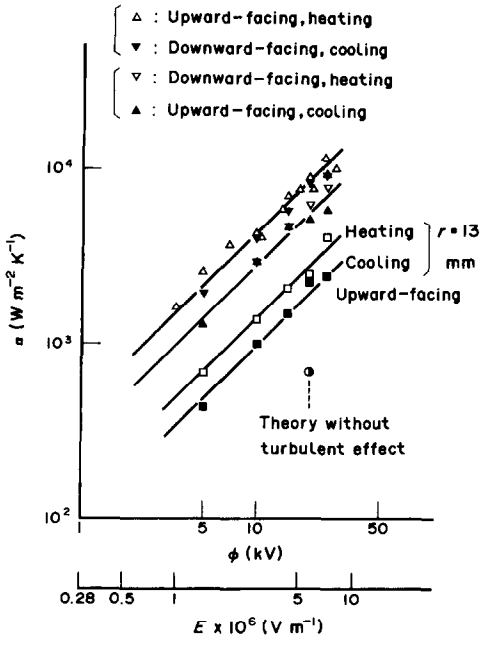

FIG. 2. Relationship between convective heat transfer coefficients and electric field.

for the cases of the upward-facing cooled plate and the downward-facing heated plate. Heat transfer coefficients at $r = 13$ mm were also augmented in proportion to the applied voltage.

As for the natural convection heat transfer without the electric field, 50 W m^{-2} K^{-1} was attained within an error of $\pm 30\%$ in the case of the upward-facing cooled plate and 6×10^2 W m^{-2} K^{-1} was attained within an error of $\pm 15\%$ in the case of the upward-facing heated plate. Based on these values, for the upward-facing heat transfer plate and an applied voltage of 20 kV, the natural convection heat transfer coefficients were increased by about 110 times in the case of cooling and by about 14 times in the case of heating. The electric power consumption to generate the EHD liquid jet was about 1.4 W (applied voltage, 20 kV; current, 70 μA).

3.2. *Effect of heat transfer on velocity distributions of the EHD liquid jet*

The velocity of the EHD liquid jet at the point 1 mm above the top of the ring electrode in the case of the upward-facing plate was increased in proportion to the applied voltage. Its value reached about 67 cm s^{-1} at the applied voltage of 25 kV independent of the temperature conditions, i.e. the heated plate, the cooled plate and the non-heated plate. Therefore, it was clarified that in the range of our experiments the heat transfer coefficients were increased in proportion to the velocity of the EHD liquid jet.

The velocity distributions in the case of an upward-facing cooled plate and in the case of a uniform temperature condition using the non-heated plate are both shown in Fig. 3 for $D = 2.5$ mm, $\Phi = 20$ kV. The velocity distributions of the EHD liquid jet above the ring electrode were nearly the same, and their maximum speeds were also nearly equal. Furthermore, the velocity distributions in the field outside of the ring electrode have nearly the same values. Therefore, it was determined that the cooling of the plate had a negligibly small influence on the velocity distribution of the EHD liquid jet. In the case of heating, the velocity distribution was compared with that for the case of a uniform temperature condition using the non-heated plate at the condition of $D = 3.5$ mm and $\Phi = 28$ kV. The maximum velocity near the axisymmetric axis had nearly equal values within an error of $\pm 10\%$. Also since the velocity distribution both inside of the electrode and in the area surrounding the ring electrode was nearly the same, the heating of the plate had a negligibly small effect on the velocity distribution of the EHD liquid jet. Consequently, it was clarified experimentally that the heating and the cooling of the plate electrode had a negligibly small influence on the velocity distribution of the EHD liquid jet.

3.3. *Turbulent intensity of the EHD liquid jet above the heat transfer surface*

As can be seen from Fig. 3, the velocity distribution is a reverse of the usual stagnation flow, where the velocity was in the opposite direction and where the flow could be called the 'reverse-stagnation flow' or the 'rear-stagnation flow'. This kind of reverse-stagnation flow was not realized easily and has not yet been clarified in detail. But as the reverse-stagnation flow had to change the direction of the flow at the axisymmetric axis and the points where $\partial^2 u_z/\partial r^2 = 0$ necessarily existed along the velocity distribution of any jet, the instability of the flow would occur easily near the axisymmetric axis or the flow would be separated at the point near $r = 0$ and $z = 0$, and that would produce the turbulence. Therefore, in this study the turbulent intensities of the EHD liquid jet along the axisymmetric axis were measured in order to find the flow characteristics of the EHD liquid jet above the heat transfer plate where turbulence could greatly affect heat transfer.

First, the turbulent intensity in the r-direction $(\overline{u_r'^2})^{0.5}$ and the z-direction $(\overline{u_z'^2})^{0.5}$ were measured for frequencies between 0.25 Hz and 2 kHz. In Fig. 4(a) the turbulent intensities at $z = 2.5$ mm above the heat transfer plate along the axisymmetric axis are shown. The turbulent intensities were increased in proportion to the applied voltage, and the turbulent intensities for the r- and z-direction were nearly equal. Furthermore, when using the heated plate, the non-heated plate and the cooled plate the turbulent intensities were clearly not changed.

In the next step, since the turbulent intensities for the r-direction and those for the z-direction were of the same magnitude, only the turbulent intensities for the r-direction, that would be able to be measured to

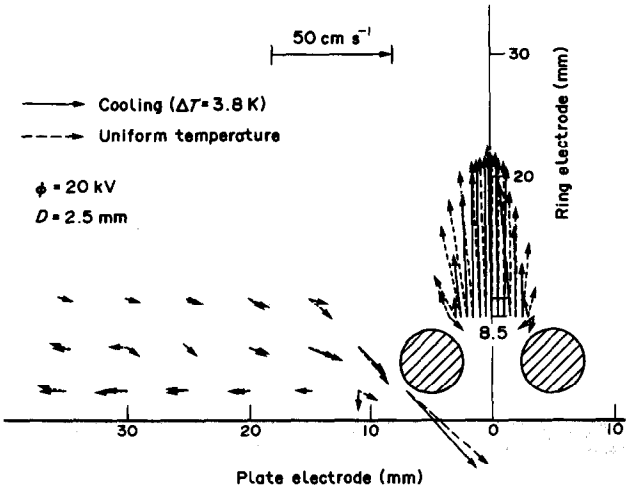

FIG. 3. Effect of heat transfer on velocity distributions of EHD liquid jet.

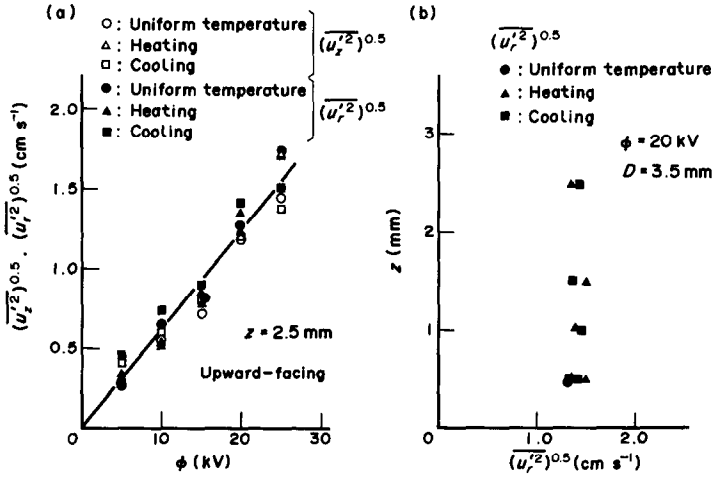

FIG. 4. (a) Relationship between turbulent intensity and electric field. (b) Turbulent intensity along vertical axis.

the point just above the heat transfer plate by LDV, were measured to the point of $z = 0.5$ mm just above the plate, as shown in Fig. 4(b). The turbulent intensities did not change along the axisymmetric axis between $z = 2.5$ and 0.5 mm above the plate, and the turbulent intensities were nearly constant, independent of the thermal condition of using the heated plate, the cooled plate and the non-heated plate. From this figure, it is clearly seen that the turbulent intensities of the EHD liquid jet are about 1.3 cm s^{-1} for the applied voltage of 20 kV, and that the turbulent intensities had nearly the same values in the area between the ring electrode and the plate electrode along the axisymmetric axis to the point of $z =$ 0.5 mm just above the plate, again independent of the thermal conditions of the plate electrode.

3.4. *Theoretical analysis of convective heat transfer augmentation by applying the EHD liquid jet*

Convective heat transfer in the EHD liquid jet was analyzed theoretically in order to estimate the heat transfer rates quantitatively. In the following analytical process, the electric field was analyzed first to determine the electric potential between the ring and the plate electrodes. Secondly, the Navier–Stokes equations with the external force based on the electric field were solved to obtain the velocity distribution. Lastly, the heat transfer augmentation by the effect of convective heat transfer of the EHD liquid jet was analyzed.

3.4.1. *Analytical model of the EHD liquid jet.* Though the net charges are zero in the case of polarization of dielectric matters, the polarized charges yielded at the stronger electric field are affected by the Coulomb force more strongly than the ones yielded at the weaker electric field. Therefore, by the resultant force which is the sum of the forces exerted on each polarized charge, the fluid element is also forced to the stronger electric field region. This force is called an electrostriction force, and is expressed as the third term of equation (1). It is simplified to $\nabla[E^2(\varepsilon-\varepsilon_0)(\varepsilon+2\varepsilon_0)/6\varepsilon_0]$ for non-polar fluids. Until

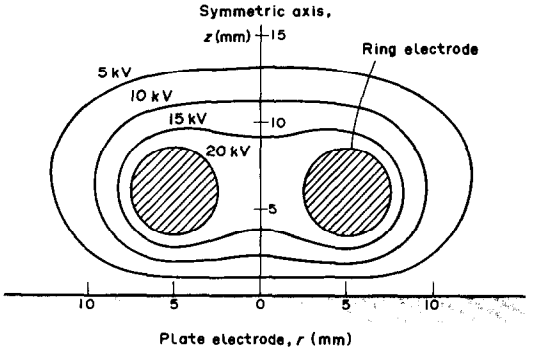

FIG. 5. Distribution of electric potential (theory).

now, any convection generated due to this electrostriction force would have not been reported. In our ring and plate electrodes arrangement the electric field is not symmetric with the vertical plane including the bottom edge of the ring electrode in the case of the upward-facing flat plate. Namely, in the outer region of the ring electrode the electrostriction force makes the bottom edge of the ring electrode attract the fluid. This is caused by the larger magnitude. But in the region inside of the ring electrode this force makes the bottom edge of the ring electrode attract the fluid. This is caused by the smaller magnitude. Therefore, due to this unsymmetrical distribution of the electrostriction force, the convection of the EHD liquid jet could occur. Then, by the forced convection of the EHD liquid jet, heat transfer augmentation can be obtained.

3.4.2. *Theoretical analysis of electric field.* The relaxation time of the electric charges can be derived as $t_c = \varepsilon/\sigma_c$ from the conservation equation of the current, the definition equation of the current, and Poisson's equation [16]. For Furonsorubu AE the relaxation time of the electric charge is 1.7 ms. On the other hand, the characteristics time for the flow, i.e. the time for the flow with the experimentally obtained velocity of 67 cm s^{-1} needed to pass through the ring electrode, was calculated to be 7.5 ms. Therefore, the relaxation time of electric charges is rather small compared with the characteristic time of the EHD liquid jet flow. Consequently, the electric field is not affected by the velocity of the flow, and the electric charges would be relaxed to nearly zero over the whole region. Furthermore, since the convective current term disappears, the electric field can be analyzed independently and the governing equation is the Laplace equation $\nabla E = 0$ derived from the conservation equation of the current. In the case of an electrode distance of $D = 3.5$ mm and an applied voltage of $\Phi = 20$ kV, the electric potential distribution was numerically calculated as shown in Fig. 5. From the figure it is clearly seen that although the voltage is high enough, the electric field strength has rather weak values around the axisymmetric axis inside of the ring electrode compared to those in the region just outside of the ring electrode.

3.4.3. *Theoretical analysis of velocity distribution.* As explained above, the electric charges were relaxed to nearly zero, which means that the Coulomb force would be zero. In the case where there is no temperature distribution, since there is no gradient for the dielectric constant, the body force exerted in the electric field reduces to only the electrostriction force, which is the third term of equation (1). By assuming incompressible flow, the governing equations, in dimensionless form, for the flow field become [17]:

Navier–Stokes equation

$$\bar{u}_r\frac{\partial \bar{u}_r}{\partial \bar{r}} + \bar{u}_z\frac{\partial \bar{u}_r}{\partial \bar{z}} = \frac{1}{Re_{\mathrm{EHDJET}}}\left[\frac{\partial}{\partial \bar{r}}\left\{\frac{1}{\bar{r}}\cdot\frac{\partial}{\partial \bar{r}}(\bar{r}\bar{u}_r)\right\} + \frac{\partial^2 \bar{u}_r}{\partial \bar{z}^2}\right] + \frac{\partial \bar{E}^2}{\partial \bar{r}} - \frac{\partial \bar{p}}{\partial \bar{r}} \quad (2)$$

$$\bar{u}_r\frac{\partial \bar{u}_z}{\partial \bar{r}} + \bar{u}_z\frac{\partial \bar{u}_z}{\partial \bar{z}} = \frac{1}{Re_{\mathrm{EHDJET}}}\left[\frac{1}{\bar{r}}\cdot\frac{\partial}{\partial \bar{r}}\left(\bar{r}\frac{\partial \bar{u}_z}{\partial \bar{r}}\right) + \frac{\partial^2 \bar{u}_z}{\partial \bar{z}^2}\right] + \frac{\partial \bar{E}^2}{\partial \bar{z}} - \frac{\partial \bar{p}}{\partial \bar{z}}. \quad (3)$$

Poisson's equation for pressure

$$\frac{\partial}{\partial \bar{r}}\left[\frac{1}{\bar{r}}\cdot\frac{\partial}{\partial \bar{r}}\{\bar{r}(\bar{p}-\bar{E}^2)\}\right] + \frac{\partial^2(\bar{p}-\bar{E}^2)}{\partial \bar{z}^2} = -2\left(\frac{\partial \bar{u}_r}{\partial \bar{z}}\right)\left(\frac{\partial \bar{u}_z}{\partial \bar{r}}\right) + 2\left(\frac{\partial \bar{u}_r}{\partial \bar{r}}\right)\left(\frac{\partial \bar{u}_z}{\partial \bar{z}}\right) + \frac{2\bar{u}_r}{\bar{r}}\left\{\left(\frac{\partial \bar{u}_r}{\partial \bar{r}}\right) + \left(\frac{\partial \bar{u}_z}{\partial \bar{z}}\right)\right\} \quad (4)$$

$$\bar{u}_r = u_r/U_{\mathrm{EHDJET}}, \quad \bar{u}_z = u_z/U_{\mathrm{EHDJET}}$$

$$U_{\mathrm{EHDJET}} = (\Phi/D)\cdot[(\varepsilon-\varepsilon_0)(\varepsilon+2\varepsilon_0)/6\varepsilon_0\rho]^{0.5}$$

$$\bar{E} = E/(\Phi/D), \quad \bar{p} = p/(\rho U^2_{\mathrm{EHDJET}}), \quad \bar{r} = r/d$$

$$\bar{z} = z/d, \quad Re_{\mathrm{EHDJET}} = U_{\mathrm{EHDJET}}\cdot d/\nu$$

where U_{EHDJET} is the characteristic velocity of the EHD liquid jet, Re_{EHDJET} the Reynolds number using U_{EHDJET} as the representative velocity, and Re_{EHDJET} is called the 'EHDJET Reynolds number' by the authors.

Since the electrostriction force is a gradient force like pressure and therefore could not produce any vorticity by itself, the flow field could be numerically calculated by using velocity components and pressure as variables. Although the existence of turbulence was already cleared from the previous experiments, upwind difference methods of the third order were utilized instead of using any turbulent model where some undetermined coefficients would remain, to clarify the mechanism of the flow basically. In the case of the electrode distance of $D = 3.5$ mm and the applied voltage of $\Phi = 20$ kV, where U_{EHDJET} was 71.4 cm s^{-1} and Re_{EHDJET} was 8.8×10^3, the numerically calculated velocity distribution is shown in Fig. 6. Figure 6 shows the jet flow pattern and the reverse flow outside of

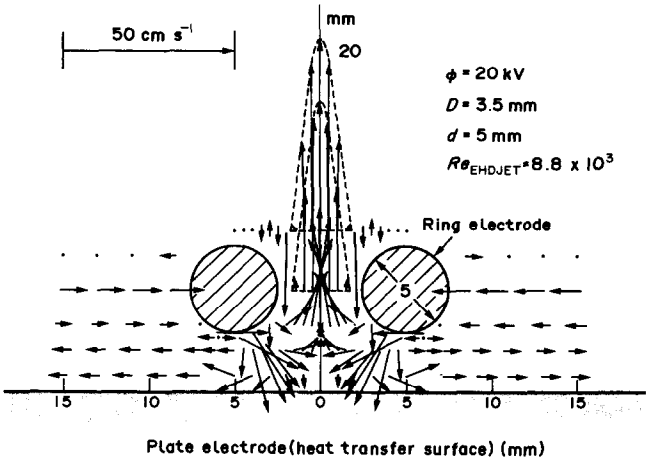

FIG. 6. Velocity distribution (theory).

the ring electrode generated like the experimentally measured velocity distributions, as shown in Fig. 3. Furthermore, the numerically calculated maximum velocity along the axisymmetric axis was 56 cm s^{-1} at $z = 9.5$ mm and was nearly equal to the measured maximum velocity of 59 cm s^{-1}. Therefore, the numerically calculated velocity distribution which coincided well with the measured velocity was obtained. Also it was clarified that the EHD liquid jet was generated by the electrostriction force.

3.4.4. *Theoretical analysis of temperature distribution.* The temperature distribution was analyzed based on the assumption that the temperature distribution was determined by the forced convection heat transfer of the EHD liquid jet with numerically calculated velocity distributions. The governing equation was normalized and is

$$\bar{u}_r \frac{\partial \bar{T}}{\partial \bar{r}} + \bar{u}_z \frac{\partial \bar{T}}{\partial \bar{z}} = \frac{1}{Re_{\mathrm{EHDJET}} \cdot Pr} \left\{ \frac{1}{\bar{r}} \cdot \frac{\partial}{\partial \bar{r}} \left(\bar{r} \frac{\partial \bar{T}}{\partial \bar{r}} \right) + \frac{\partial^2 \bar{T}}{\partial \bar{z}^2} \right\} \tag{5}$$

where $\bar{T} = T/\Delta T$. By calculating with a fine mesh of 0.05 mm near the wall and by using the upwind difference methods of first order at $Pr = 8.3$, the numerically calculated heat transfer coefficients were $\alpha = 700$ W m^{-2} K^{-1}. This value was lower by one order of magnitude than the actually attained heat transfer coefficients. Therefore, it was found that a theoretical analysis without considering the turbulent effect was not able to predict the actual high heat transfer coefficients.

3.4.5. *Estimation of turbulent heat flux by considering the turbulent intensity.* From the numerical analysis, it was shown that the turbulent effect was important in the heat transfer of the EHD liquid jet. Therefore, by using the measured turbulent intensity, the magnitude of the turbulent heat flux was estimated. Namely, by using the eddy viscosity for modelling the Reynolds stress and by assuming the turbulent Prandtl number of 0.9, the turbulent intensity was correlated with the exchange coefficients as follows:

$$\rho \overline{u_r' u_z'} \fallingdotseq \rho \varepsilon_t (\partial u/\partial z) \fallingdotseq (0.9) \rho \varepsilon_q (\partial u/\partial z). \tag{6}$$

By assuming

$$\overline{u_r' u_z'} = |\overline{u_r'}| \cdot |\overline{u_z'}| = (\overline{u_r'^2})^{0.5} \cdot (\overline{u_z'^2})^{0.5}$$

$$\partial u/\partial z = U_{\mathrm{EHDJET}}/d$$

in order to estimate the order of magnitude, ε_q became 0.013 cm^2 s^{-1}. The ratio of this exchange coefficient of turbulent heat flux to the thermal conductivity was calculated as $\rho c_p \varepsilon_q / \lambda = 27 = O(10)$. Therefore, it was estimated that the turbulent heat flux was larger by one order of magnitude than the heat flux without considering turbulent effects. Since this difference of magnitude coincided with the fact that the theoretical results without considering the turbulent effects were one order of magnitude smaller than the experimental results, it was estimated that the experimental values would be able to be quantitatively explained by the turbulent effects.

Concerning the difference between the heat transfer coefficients obtained experimentally for the cases using the heated plate and the cooled plate, the cause has not yet been determined from the experiments and the theoretical analysis carried out so far. But the thickness of the thermal boundary layer was estimated to be of the order of 0.1 mm by the theoretical analysis. Therefore, measuring several turbulent characteristics, such as turbulent intensity to about $z = 0.1$ mm just above the heat transfer surface, would help to clarify the mechanism of the difference of heat transfer coefficients obtained between the cases of the heating condition and the cooling condition.

4. AUGMENTATION OF BOILING HEAT TRANSFER BY APPLYING THE EHD LIQUID JET

Since the EHD liquid jet has the potential to augment the boiling heat transfer by forced convection

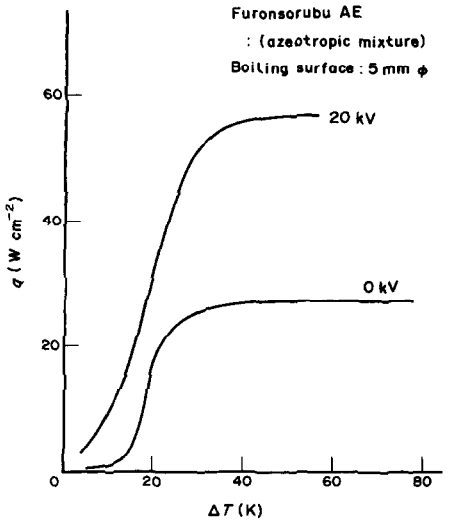

FIG. 7. Augmentation of boiling heat transfer by applying EHD liquid jet.

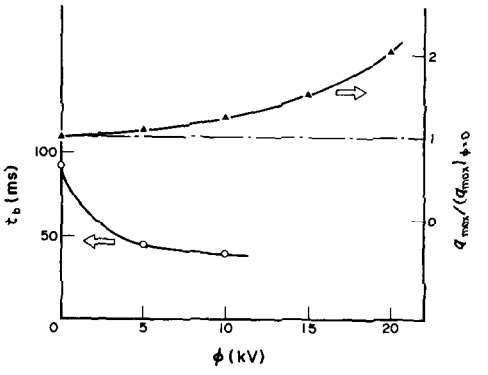

FIG. 8. Augmentation of critical heat flux and mean bubble detachment period.

and to enhance the bubble detachment from the surface, augmentation experiments have been conducted for the azeotropic mixture of R 113 and ethanol. The boiling curves of Furonsorubu AE are shown in Fig. 7. The boiling curve representing no electric field did not decline in the transition boiling region, and may be one of the characteristics of the boiling of azeotropic mixtures. The critical heat flux corresponding to the curve representing no electric field was 27 ± 3 W cm^{-2}. When an electric field of 20 kV was applied for an electrode distance of 3.5 mm, the critical heat flux was increased by 2.1 times to attain 57 ± 8 W cm^{-2}. Considering the boiling curve for 20 kV, in the natural convection region of the wall superheat (below about 10 K), heat transfer was enhanced over ten times by forced convection. In the nucleate boiling region the heat transfer augmentation was attained over 1.8 times and was greatly enhanced for the smaller values of wall superheat. Furthermore, since the wall superheat corresponding to the onset of the critical heat flux increased 10 K more than the one without an electric field, it was clear that the occurrence of the critical heat flux was depressed until the larger wall superheat by applying the EHD liquid jet.

In order to clarify the mechanism of boiling heat transfer enhancement, the mean bubble detachment period was measured and is shown in Fig. 8. From the figure, it is seen that the mean bubble detachment period decreased according to the increase of the applied voltage until the applied voltage of 10 kV. Especially, the extremely long bubble detachment periods of 100–300 ms that were often observed in the case not using an electric field almost completely disappeared when an electric field was applied. Therefore, it was clear that an important reason for the heat transfer enhancement was that the bubble detachment period was shortened by applying the EHD liquid jet. But in the cases of applying 15 and 20 kV, since the critical wavelength for Taylor instability became shorter than the diameter of the boiling heat transfer surface, the motion of the bubbles and the behavior of the vapor–liquid interface were too fast and too complicated to measure the mean bubble detachment period. However, the relationship between the enhancement of the critical heat flux and the applied voltage is also shown in Fig. 8. The enhancement of the critical heat flux increased according to the increase of the applied voltage.

5. ENHANCEMENT OF CONVECTIVE HEAT TRANSFER BY APPLYING MULTI-SETS OF THE EHD LIQUID JET

In order to apply the EHD liquid jet to a wider heat transfer surface, the enhancement of convective heat transfer using multi-sets of the EHD liquid jet was experimentally investigated. In such cases, utilizing a non-uniform mesh, which was made by extracting some wires from a uniform wire mesh, would be preferable to setting the many ring electrodes with the same electrode distance between the ring and the plate. Then, a number of EHD liquid jets would occur from the many areas surrounded by the wire mesh. Furthermore, a perforated plate electrode, which has two alternating types of holes corresponding to the different diameters, would also be effective.

In this paper, as a fundamental study to develop the larger application electrodes such as the non-uniform wire mesh or the perforated plate, multi-sets of twin straight wires were used to clarify the effect of multi-sets of twin wires by generating the two-dimensional EHD liquid jet. The parameters of the experiment were the diameter of the wire d, the distance between wire electrodes (W_s was the shorter distance and W_l was the longer distance), and the electrode distance D between the wires and the plate.

5.1. *Twin wire electrodes*

A two-dimensional EHD liquid jet was obtained for D/d values less than about 1.0 with $1 \leqslant d \leqslant 5$ mm and $W_s/d \fallingdotseq 1$. For D/d values which are larger than about 1.5, an EHD liquid jet could not be generated.

5.2. *Multi-sets of twin wire electrodes*

By using three sets of twin wire electrodes with the same distance between neighboring twin wire electrodes, the EHD liquid jet was generated similar to the case of one set of twin wire electrodes for D/d values less than about 1.0. In this case the liquid was ejected from the smaller gap of the wire electrodes and was sucked into the interior region between the electrodes, through the larger gap of wire electrodes (range of experiments, $0.2 \leqslant W_s/d \leqslant 5$).

However, for D/d values larger than about 1.5, the EHD liquid jet was generated in contrast to the case of one set of twin wire electrodes. Furthermore, the direction of flow was completely opposite, compared to the case where D/d was smaller than about 1.0. Namely, the EHD liquid jet was ejected from the larger gap between wire electrodes and was sucked into the interior region between the wire and plate electrodes through the smaller gap. The mechanism of this phenomenon is considered as follows. Even though D/d was larger than 1.5, the twin wire electrodes acted as if they were only one wire electrode with a larger diameter, when considered from the viewpoint of the distribution of electric field strength. Then, the equivalent value of D/d for this electrode arrangement would be decreased to a value of less than about 1.0. Therefore, the EHD liquid jet was generated and ejected from the larger gap between wire electrodes (range of experiments, $2 \leqslant W_l/d \leqslant 25$, $W_s/d \fallingdotseq 1$). In the cases of utilizing the non-uniform wire mesh electrode composed of wire 1 mm in diameter and the 1 mm thick perforated plate electrode with an electrode distance larger than 1.5 mm, this kind of EHD liquid jet occurred and jets were ejected from the larger sections or larger holes and the liquid was sucked into the smaller sections or smaller holes.

Since this kind of EHD liquid jet would be especially important from the application standpoint, the heat transfer coefficients were measured for the electrodes arrangement of $d = 1$ mm, $W_s = 1$ mm, $W_l = 5$ mm, $D = 1.5$–2.0 mm as shown in Fig. 9. The heat transfer coefficients were measured at two points as shown in the figure. Case A was measured just over the twin wire electrodes, where the flow was sucked into the interior region between the electrodes. Case B was measured at the larger gap between the wire electrodes, where the jet was ejected from the heat transfer surface. The experiments were performed with the downward-facing cooled plate, and the heat transfer coefficients obtained for case A were larger by 30% than those for case B. The absolute values of the heat transfer coefficients obtained were nearly equal to those obtained in Fig. 2, when compared for the same characteristic electric field strength.

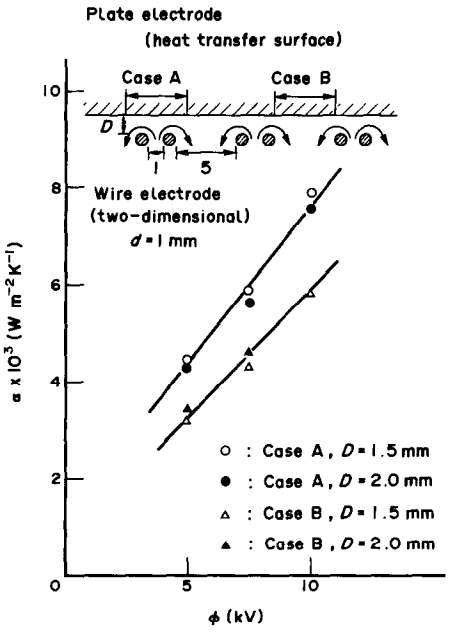

FIG. 9. Convective heat transfer augmentation by applying multi-sets of EHD liquid jet.

6. CONCLUSIONS

As a fundamental study of EHD augmentation methods of heat transfer in liquids, an EHD liquid jet, which was recently observed by the authors for the electrode arrangement composed of a ring electrode and a parallel opposed plate electrode, was applied in the azeotropic mixture of R 113 and ethanol. The following conclusions were obtained experimentally and theoretically for the enhancement of convective and boiling heat transfer.

(1) Convective heat transfer coefficients from the plate have been increased in proportion to the electric field strength due to the effect of the EHD liquid jet. Compared to the natural convection heat transfer coefficients, the heat transfer coefficients were enhanced, at the maximum over 100 times. It was experimentally clarified that the heat transfer coefficients realized in the cases of the upward-facing heated plate and the downward-facing cooled plate were greater by about 50% than those for the cases of the upward-facing cooled plate and the downward-facing heated plate.

(2) Although the theoretical analysis based on the electrostriction force has been able to quantitatively explain the experimental velocity distribution of the EHD liquid jet, the theoretical analysis without considering the turbulent effects could not quantitatively explain the enhanced convective heat transfer coefficients. Therefore, it was clear that the turbulent heat flux due to the turbulent intensity of the EHD liquid jet was important.

(3) Boiling heat transfer was enhanced for both regions of nucleate and transition boiling by applying the EHD liquid jet to attain the critical heat flux augmented over two times. It was also experimentally clear that the bubble detachment period was decreased by the effect of the EHD liquid jet.

(4) By using the multi-sets of twin wire electrodes,

it was clarified experimentally that for values of (electrode distance/wire diameter) less than about 1.0, the liquid was ejected from the smaller gap of wire electrodes, but that for values of (electrode distance/wire diameter) larger than about 1.5, the liquid was ejected from the larger gap of wire electrodes.

Acknowledgements—The authors want to express their sincere gratitude to Mr M. Iguchi, Mr T. Taketani and M. K. Kikuchi of the Mechanical Engineering Laboratory, and to Mr C. Goto and Mr N. Wakayama of the Science University of Tokyo, for their assistance in making the experimental apparatus and in carrying out the experiments. Also the authors wish to thank Prof. Y. Mori of the University of Electro-Communications and Prof. K. Hijikata of the Tokyo Institute of Technology, for their wonderful advice and fruitful discussions. Numerical calculations in this paper were carried out by using the M380 Computer of RIPS Center of Agency of Industrial Science and Technology, MITI. The computing time was about 30 min.

REFERENCES

1. F. A. Kulacki, Augmentation of low Reynolds number forced convection channel flow by electrostatic discharge. In *Low Reynolds Number Flow Heat Exchangers* (Edited by S. Kakac, R. K. Shah and A. E. Bergles), pp. 753–782. Hemisphere, Washington, DC (1983).
2. A. Yabe, Y. Mori and K. Hijikata, EHD study of the corona wind between wire and plate electrodes, *AIAA J.* **16,** 340–345 (1978).
3. A. Yabe, Y. Mori and K. Hijikata, Heat transfer augmentation around a downward-facing flat plate by non-uniform electric fields, *Proc. 6th Int. Heat Transfer Conf.*, Vol. 3, pp. 171–176 (1978).
4. A. Yabe, K. Kikuchi, T. Taketani, Y. Mori and K. Hijikata, Augmentation of condensation heat transfer by applying non-uniform electric fields, *Proc. 7th Int. Heat Transfer Conf.*, Vol. 5, pp. 189–194 (1982).
5. A. Yabe, K. Kikuchi, T. Taketani, Y. Mori and H. Maki, Augmentation of condensation heat transfer by applying electro-hydro-dynamical pseudo-dropwise condensation, *Proc. 8th Int. Heat Transfer Conf.*, Vol. 6, pp. 2957–2962 (1986).
6. A. Yabe, Y. Mori and K. Hijikata, Heat transfer enhancement techniques utilizing electric fields. In *Heat Transfer in High Technology and Power Engineering* (Edited by W. J. Yang and Y. Mori), pp. 394–405. Hemisphere, Washington, DC (1987).
7. A. Yabe, T. Taketani, K. Kikuchi, Y. Mori and K. Hijikata, Augmentation of condensation heat transfer around vertical cooled tubes provided with helical wire electrodes by applying non-uniform electric fields. In *Heat Transfer Science and Technology* (Edited by Bu-Xuan Wang), pp. 812–819. Hemisphere, Washington, DC (1987).
8. J. Berghmans, Electrostatic fields and the maximum heat flux, *Int. J. Heat Mass Transfer* **19,** 791–797 (1976).
9. P. H. G. Allen and P. Cooper, The potential of electrically enhanced evaporators, *Proc. 3rd Int. Symp. on the Large Scale Applications of Heat Pumps*, pp. 221–229 (1987).
10. S. Ogata, K. Ten, K. Nishijima and J. S. Chang, Development of improved bubble disruption and dispersion technique by an applied electric field method, *A.I.Ch.E. Jl* **31,** 62–69 (1985).
11. T. B. Jones, Electrohydrodynamically enhanced heat transfer in liquids—a review. In *Advances in Heat Transfer*, Vol. 14, pp. 107–148. Academic Press, New York (1978).
12. O. M. Stuetzer, Ion drag pumps, *J. Appl. Phys.* **31,** 136–146 (1960).
13. R. J. Turnbull, Free convection from a heated vertical plate in a direct-current electric field, *Physics Fluids* **12,** 2255–2263 (1969).
14. T. Fujino and Y. H. Mori, The effect of a transverse electric field on laminar channel flow with constant heat rate, *Proc. 4th Int. Symp. on Flow Visualization*, pp. 643–648 (1986).
15. A. Castellanos, P. Atten and M. G. Velarde, Oscillatory and steady convection in dielectric liquid layers subjected to unipolar injection and temperature gradient, *Physics Fluids* **27,** 1607–1615 (1984).
16. W. K. H. Panofsky and M. Phillips, *Classical Electricity and Magnetism*, Chaps 6 and 7. Addison-Wesley, Reading, Massachusetts (1962).
17. A. Yabe and Y. Mori, Experimental and theoretical study of electro-hydrodynamical liquid jet between ring and plate electrodes (unpublished).
18. A. Yabe, M. Iguchi, T. Taketani and K. Kikuchi, Augmentation mechanism of burnout heat flux by applying electric fields (1st report, latent heat flux and its enhancement by electric fields), *Proc. 1987 ASME-JSME Thermal Engineering Joint Conference*, Vol. 4, pp. 417–424 (1987).

AUGMENTATION DU TRANSFERT THERMIQUE PAR EBULLITION ET PAR CONVECTION EN APPLIQUANT UN JET LIQUIDE ELECTRO-HYDRODYNAMIQUE

Résumé—L'effet d'accroissement d'un jet liquide électro-hydrodynamique (EHD) sur le transfert thermique de convection et d'ébullition est analysé expérimentalement et théoriquement. Le jet liquide EHD qui sort à travers une électrode annulaire en s'éloignant de la plaque est produit en appliquant une tension électrique très élevée entre l'électrode et la plaque. Le transfert de chaleur par convection sur la plaque est augmenté de 100 fois en convection forcée avec l'effet du jet liquide EHD sur la turbulence. Pour le transfert thermique par ébullition, la période moyenne de détachement des bulles diminue et le flux critique thermique est accru plus de deux fois.

ERHÖHUNG DES WÄRMEÜBERGANGS BEI KONVEKTION UND BEIM SIEDEN DURCH ANWENDUNG EINES ELEKTRO-HYDRODYNAMISCHEN FLÜSSIGKEITSSTRAHLS

Zusammenfassung—Der Einfluß eines elektro-hydrodynamischen (EHD) Flüssigkeitsstrahls auf die Erhöhung des Wärmeübergangs bei Konvektion und beim Sieden wurde experimentell und theoretisch untersucht. Der EHD-Flüssigkeitsstrahl wurde durch Anlegen einer hohen elektrischen Spannung zwischen Ringelektrode und Plattenelektrode von der Platte weg ausgestoßen. Der konvektive Wämeübergang an der Plattenelektrode wurde um mehr als das Hundertfache durch die erzwungene Konvektion und die Turbulenzeinflüsse des EHD-Flüssigkeitsstrahls erhöht. Beim Sieden nahm die mittlere Blasenablösezeit ab, und die kritische Wärmestromdichte wurde um mehr als das Doppelte erhöht.

ИНТЕНСИФИКАЦИЯ КОНВЕКТИВНОГО ТЕПЛООБМЕНА И ТЕПЛООБМЕНА ПРИ КИПЕНИИ ЗА СЧЕТ ЭЛЕКТРО-ГИДРОДИНАМИЧЕСКОЙ СТРУИ ЖИДКОСТИ

Аннотация—Экспериментально и теоретически изучалась интенсификация за счет электрогидродинамической (ЭГД) струи жидкости на конвективный теплообмен и теплообмен при кипении. ЭГД струя жидкости, вытекающая из кольцевого электрода в направлении от пластины, создавалась приложением высокого электрического напряжения между кольцевым и пластинчатым электродами. Конвективный теплоперенос от пластинчатого электрода увеличивался более, чем в 100 раз за счет вынужденной конвекции и турбулентных эффектов ЭГД струи жидкости. При теплообмене при кипении средний период отрыва пузырька был уменьшен, а величина критического теплового потока увеличена более, чем вдвое.